eprints@whiterose.ac.uk
https://eprints.whiterose.ac.uk/

Voltage stability and reactive power sharing in inverter-based microgrids with consensus-based distributed voltage control

Johannes Schiffer, Thomas Seel, Jörg Raisch, Tevfik Sezi

Abstract—We propose a consensus-based distributed voltage control (DVC), which solves the problem of reactive power sharing in autonomous inverter-based microgrids with dominantly inductive power lines and arbitrary electrical topology. Opposed to other control strategies available thus far, the control presented here does guarantee a desired reactive power distribution in steady-state while only requiring distributed communication among inverters, i.e., no central computing nor communication unit is needed. For inductive impedance loads and under the assumption of small phase angle differences between the output voltages of the inverters, we prove that the choice of the control parameters uniquely determines the corresponding equilibrium point of the closed-loop voltage and reactive power dynamics. In addition, for the case of uniform time constants of the power measurement filters, a necessary and sufficient condition for local exponential stability of that equilibrium point is given. The compatibility of the DVC with the usual frequency droop control for inverters is shown and the performance of the proposed DVC is compared to the usual voltage droop control [1] via simulation of a microgrid based on the CIGRE (Conseil International des Grands Réseaux Electriques) benchmark medium voltage distribution network.

Index Terms—Microgrid control, microgrid stability, voltage stability, smart grid applications, inverters, droop control, power sharing, secondary control, consensus algorithms, multi-agent systems, distributed cooperative control.

I. INTRODUCTION

Microgrids represent a promising concept to facilitate the integration of distributed renewable sources into the electrical grid [2]–[4]. Two main motivating facts for the need of such concepts are: *(i)* the increasing installation of renewable energy sources world-wide – a process motivated by political, environmental and economic factors; *(ii)* a large portion of these renewable sources consists of small-scale distributed generation units connected at the low (LV) and medium voltage (MV) levels via AC inverters. Since the physical characteristics of inverters largely differ from the characteristics of conventional electrical generators, i.e., synchronous generators (SGs), different control approaches are required [5].

A microgrid addresses these issues by gathering a combination of generation units, loads and energy storage elements at distribution level into a locally controllable system, which can be operated either in grid-connected mode or in islanded mode, i.e., in a completely isolated manner from the main transmission system.

J. Schiffer and T. Seel are with the Technische Universität Berlin, Germany {schiffer, seel}@control.tu-berlin.de

J. Raisch is with the Technische Universität Berlin & Max-Planck-Institut für Dynamik komplexer technischer Systeme, Germany raisch@control.tu-berlin.de

T. Sezi is with Siemens AG, Smart Grid Division, Nuremberg, Germany tevfik.sezi@arcor.de

Essential components in power systems are so-called grid-forming units. In AC networks, these units have the task to provide a synchronous frequency and a certain voltage level at all buses in the network, i.e., to provide a stable operating point. Analyzing under which conditions such an operating point can be provided and maintained, naturally leads to the problems of frequency and voltage stability. In conventional power systems, grid-forming units are SGs. In inverter-based microgrids, however, grid-forming capabilities have to be provided by inverter-interfaced sources [6], [7]. Inverters operated in grid-forming mode can be represented as ideal AC voltage sources [5]–[9].

Besides frequency and voltage stability, power sharing is an important performance criterion in the operation of microgrids [5]–[8]. Here, power sharing is understood as the ability of the local controls of the individual generation sources to achieve a desired steady-state distribution of the power outputs of all generation sources *relative* to each other, while satisfying the load demand in the network. The relevance of this control objective lies within the fact that it allows to prespecify the utilization of the generation units in operation, e.g., to prevent overloading [7].

In conventional power systems, where generation sources are connected to the network via SGs, droop control is often used to achieve the objective of active power sharing [10]. Under this approach, the current value of the rotational speed of each SG in the network is monitored locally to derive how much power each SG needs to provide.

Inspired hereby, researchers have proposed to apply a similar control to AC inverters [1], [11]. It has been shown – in [12], [13] for lossless microgrids and in [14] for lossy networks – that this heuristic proportional decentralized control law indeed locally stabilizes the network frequency and that the control gains and setpoints can be chosen such that a desired active power distribution is achieved in steady-state without any explicit communication among the different sources. The nonnecessity of an explicit communication system is explained by the fact that the network frequency serves as a common implicit communication signal. Since the actuator signal of this control is the local frequency, it is called *frequency droop control* throughout the present paper.

Furthermore, in large transmission systems droop control is usually only applied to obtain a desired active power distribution, while the voltage amplitude at a generator bus is regulated to a nominal voltage setpoint via an automatic voltage regulator (AVR) acting on the excitation system of the SG. In microgrids the power lines are typically relatively short. Then, the AVR employed at the transmission level is in general not appropiate since even slight differences in voltage amplitudes (caused, e.g., by sensor inaccuracies) can provoke

high reactive power flows [15]. Therefore, droop control is typically also applied to the voltage with the objective to achieve a desired reactive power distribution in microgrids. The most common (heuristic) approach is to set the voltage amplitude via a proportional control, the feedback signal of which is the reactive power generation relative to a reference setpoint [1], [9]. Hence, we call this control *voltage droop control* throughout the paper.

The droop control strategies discussed previously are derived under the assumption of a dominantly inductive network, i.e., for power lines with small R/X ratios, and they are (by far) the most commonly used ones in this scenario [9]. However, even in networks with dominantly inductive power lines, the voltage droop control [1] exhibits a significant drawback: it does in general not guarantee a desired reactive power sharing, i.e., it does, in general, not achieve the desired control goal, as discussed e.g., in [13], [16]–[18]. Moreover, to the best of the authors' knowledge, no theoretically or experimentally well-founded selection criteria are known for the parameters of the voltage droop control that would ensure at least a guaranteed minimum (quantified) performance in terms of reactive power sharing.

As a consequence, several other or modified (heuristic) decentralized voltage control strategies have been proposed in the literature, e.g., [16]–[22]. Most of this work is restricted to networks of inverters connected in parallel. Moreover, typically only networks composed of two DG units are considered. Conditions on voltage stability for a parallel inductive microgrid with constant power loads have been presented in [18]. With most approaches the control performance in terms of reactive power sharing with respect to the original control [1] is improved. However, no general conditions or formal guarantees for reactive power sharing are given. A quantitative analysis of the error in power sharing is provided in [16] for the control proposed therein.

Other related work is [23], in which several local and centralized control schemes for reactive power control of photovoltaic units are compared via simulation with respect to voltage regulation and loss minimization. In [24], [25], distributed control schemes for the problem of optimal reactive power compensation are presented. Therein, the distributed generation (DG) units are modeled as constant power or P-Q buses and, hence, assumed to be operated as grid-feeding and not as grid-forming units [6], [8]. In [24], loads are modeled by the exponential model, while in [23], [25], constant power loads are considered.

The main contributions of the present paper are two-fold: First, as a consequence of the preceding discussion, we propose a consensus-based distributed voltage control (DVC), which guarantees reactive power sharing in meshed inverter-based microgrids with dominantly inductive power lines and arbitrary electrical topology. Opposed to most other related communication-based control concepts, e.g., [26], [27], the present approach does only require distributed communication among inverters, i.e., it does neither require a central communication or computing unit nor all-to-all communication among the inverters.

The consensus protocol used to design the DVC is based on the weighted average consensus protocol [28]. This protocol has been applied previously in inverter-based microgrids to the problems of secondary frequency control [12], [29]–[31], as well as secondary voltage control [30]–[33]. In contrast to the approach of the present paper, the secondary voltage control scheme proposed in [30], [31] is designed to regulate all voltage amplitudes to a common reference value. As a consequence, this approach does, in general, not achieve reactive power sharing.

Second, unlike other work on distributed voltage control considering reactive power sharing, e.g., [32]–[34], we provide a rigorous mathematical analysis of the closed-loop voltage and reactive power dynamics of a microgrid with inductive impedance loads under the proposed DVC. More precisely, we prove that the choice of the control parameters uniquely determines the corresponding equilibrium point. In addition, for the case of uniform time constants of the power measurement filters, we give a necessary and sufficient condition for local exponential stability of that equilibrium point. The two latter results are derived under the standard assumption of small phase angle differences between the output voltages of the DG units [10], [18].

Furthermore, and as discussed previously, the performance of the voltage droop control [1] in terms of reactive power sharing is, in general, unsatisfactory. Therefore, the control presented here is meant to replace the voltage droop control [1] rather than complementing it in a secondary control-like manner, as e.g., in [27], [32]–[34].

We also provide a selection criterion for the control parameters, which not only ensures reactive power sharing, but also that the average of all voltage amplitudes in the network is equivalent to the nominal voltage amplitude for all times. Finally, we evaluate the performance of the DVC compared to the voltage droop control [1] and its compatibility with the standard frequency droop control [1] via extensive simulations. Hence, the present work extends our previous results in [35] in several regards.

We would like to emphasize that reactive power sharing by manipulation of the voltage amplitudes is of particular practical interest in networks or clusters of networks, where the generation units are in close electrical proximity. This is often the case in microgrids and we only consider such networks in this paper. Then, the line impedances are relatively low, which from the standard power flow equations [10], implies that small variations in the voltage suffice to achieve a desired reactive power sharing. Also, close electrical proximity usually implies close geographical distance between the different units, which facilitates the practical implementation of a distributed communication network.

The remainder of this paper is outlined as follows: at first, we introduce the basic models of the electrical microgrid, including that of an AC inverter, and the communication network in Section II. In Section III we formalize the concept of power sharing and present the suggested DVC. The results on existence and uniqueness properties of equilibria of the closed-loop dynamics under the DVC are given in Section IV. The stability result is presented in Section V. The control performance is illustrated by simulations in Section VI. Fi-

nally, conclusions and directions for future work are given in Section VII.

II. PRELIMINARIES AND NOTATION

We define the sets $\mathcal{N} := \{1, \ldots, n\}$, $\mathbb{R}_{\geq 0} := \{x \in \mathbb{R} | x \geq 0\}$, $\mathbb{R}_{>0} := \{x \in \mathbb{R} | x > 0\}$, $\mathbb{R}_{<0} := \{x \in \mathbb{R} | x < 0\}$ and $\mathbb{T} := [0, 2\pi)$. For a set $\mathcal{V}$, let $|\mathcal{V}|$ denote its cardinality. Let $\mathcal{V}$ be a finite set of distinct natural numbers $v_i \in \mathbb{N}$, $i = 1, \ldots, |\mathcal{V}|$. Then $i \sim \mathcal{V}$ denotes "$i = v_1, \ldots, v_{|\mathcal{V}|}$". Let $x := \mathrm{col}(x_i) \in \mathbb{R}^n$ denote a vector with entries x_i, $i \sim \mathcal{N}$; $\underline{0}_n \in \mathbb{R}^n$ the vector of all zeros; $\underline{1}_n \in \mathbb{R}^n$ the vector with all ones; I_n the $n \times n$ identity matrix; $0_{n \times n}$ the $n \times n$ matrix of all zeros and $\mathrm{diag}(a_i), i \sim \mathcal{N}$, an $n \times n$ diagonal matrix with entries a_i. Furthermore, $\| \cdot \|_1$ denotes the vector 1-norm and $\| \cdot \|_\infty$ the vector ∞-norm. For $z \in \mathbb{C}$, $\Re(z)$ denotes the real part of z and $\Im(z)$ its imaginary part. Let j denote the imaginary unit. The conjugate transpose of a vector v is denoted by v^*. For a matrix $A \in \mathbb{R}^{n \times n}$, let $\sigma(A) := \{\lambda \in \mathbb{C} : \det(\lambda I_n - A) = 0\}$ denote its spectrum. The numerical range or field of values of A is defined as $W(A) := \{x^* A x : x \in \mathbb{C}^n, x^* x = 1\}$. It holds that $\sigma(A) \subseteq W(A)$ [36]. If A is symmetric then $W(A) \subseteq \mathbb{R}$ and $\min(\sigma(A)) \leq W(A) \leq \max(\sigma(A))$ [36]. Let $A_{\mathrm{sy}} = \frac{1}{2}(A + A^T)$, respectively $A_{\mathrm{sk}} = \frac{1}{2}(A - A^T)$ be the symmetric, respectively skew-symmetric part of A. Then $\Re(W(A)) = W(A_{\mathrm{sy}})$ and $\Im(W(A)) = W(A_{\mathrm{sk}})$ [36].

The following result is used in the paper.

Lemma II.1. *[36] Let A and B be matrices of appropriate dimensions and let B be positive semidefinite. Then,*

$$\sigma(AB) \subseteq W(A)W(B) := \{\lambda = \alpha\beta | \alpha \in W(A), \beta \in W(B)\}.$$

We briefly recall some graph theoretic notions used in the paper. For further information on graph theory, the reader is referred to, e.g., [37] and references therein.

An undirected graph of order n is a tuple $\mathcal{G} := (\mathcal{V}, \mathcal{E})$, where $\mathcal{V} := \{1, \ldots, n\}$ is the set of nodes and $\mathcal{E} \subseteq \mathcal{V} \times \mathcal{V}$, $\mathcal{E} := \{e_1, \ldots, e_m\}$ is the set of undirected edges. The l-th edge connecting nodes i and k is denoted as $e_l = \{i, k\} = \{k, i\}$. The set of neighbors of a node i is denoted by $\mathcal{C}_i$ and contains all k for which $e_l = \{i, k\} \in \mathcal{E}$.

The $|\mathcal{V}| \times |\mathcal{V}|$ adjacency matrix $\mathcal{A}$ has entries $a_{ik} = a_{ki} = 1$ if an edge between i and k exists and $a_{ik} = 0$ otherwise. The degree of a node i is given by $d_i = \sum_{k=1}^n a_{ik}$. With $\mathcal{D} := \mathrm{diag}(d_i) \in \mathbb{R}^{n \times n}$, the Laplacian matrix of an undirected graph is given by $\mathcal{L} := \mathcal{D} - \mathcal{A}$ and is symmetric positive semidefinite [37].

A path in a graph is an ordered sequence of nodes such that any pair of consecutive nodes in the sequence is connected by an edge. $\mathcal{G}$ is called connected if for all pairs $(i, k) \in \mathcal{V} \times \mathcal{V}$, $i \neq k$, there exists a path from i to k. Given an undirected graph, zero is a simple eigenvalue of its Laplacian matrix $\mathcal{L}$ if and only if the graph is connected. Moreover, a corresponding right eigenvector to this simple zero eigenvalue is then $\underline{1}_n$, i.e., $\mathcal{L}\underline{1}_n = \underline{0}_n$ [37].

A. Network model

This work is mainly concerned with reactive power. According to [10], [38], in lack of detailed knowledge of the load composition in the network, the most commonly accepted static load representation is to model the reactive power demand by a constant impedance. Therefore, we consider a generic meshed microgrid and assume that loads are modeled by constant impedances[1]. This leads to a set of nonlinear differential-algebraic equations (DAE). Then, a network reduction (called Kron-reduction [10]) is carried out to eliminate all algebraic equations corresponding to loads and to obtain a set of differential equations. We assume this process has been carried out and work with the Kron-reduced network.

In the reduced network, each node represents a DG unit interfaced via an AC inverter. The set of nodes of this network is denoted by $\mathcal{N} := \{1, \ldots, n\}$. We associate a time-dependent phase angle $\delta_i : \mathbb{R}_{\geq 0} \to \mathbb{T}$ and a voltage amplitude $V_i : \mathbb{R}_{\geq 0} \to \mathbb{R}_{>0}$ to each node $i \in \mathcal{N}$ in the microgrid. Two nodes i and k of the microgrid are connected via a complex admittance $Y_{ik} = Y_{ki} \in \mathbb{C}$. For convenience, we define $Y_{ik} := 0$ whenever i and k are not directly connected via an admittance. We denote the set of neighbors of a node $i \in \mathcal{N}$ by $\mathcal{N}_i := \{k \mid k \in \mathcal{N}, k \neq i, Y_{ik} \neq 0\}$. For ease of notation, we write angle differences as $\delta_{ik}(t) := \delta_i(t) - \delta_k(t)$.

We assume that the microgrid is connected, i.e., that for all pairs $\{i, k\} \in \mathcal{N} \times \mathcal{N}$, $i \neq k$, there exists an ordered sequence of nodes from i to k such that any pair of consecutive nodes in the sequence is connected by a power line represented by an admittance. This assumption is reasonable for a microgrid, unless severe line outages separating the system into several disconnected parts occur.

Furthermore, we assume that the power lines of the microgrid are *lossless*, i.e., all lines can be represented by purely inductive admittances. This may be justified as follows [12], [13]. In medium (MV) and low voltage (LV) networks the line impedance is usually not purely inductive, but has a non-negligible resistive part. On the other hand, the inverter output impedance is typically inductive (due to the output inductor and/or the possible presence of an output transformer). Under these circumstances, the inductive parts dominate the resistive parts in the admittances for some particular microgrids, especially on the MV level. We only consider such microgrids and absorb the inverter output admittance (together with a possible transformer admittance) into the line admittances Y_{ik}, while neglecting all resistive effects.

Then, an admittance connecting two nodes i and k can be represented by $Y_{ik} := jB_{ik}$ with $B_{ik} = B_{ki} \in \mathbb{R}_{<0}$. The representation of loads as constant impedances in the original network leads to shunt-admittances at at least some of the nodes in the Kron-reduced network, i.e., $\hat{Y}_{ii} = G_{ii} + j\hat{B}_{ii} \neq 0$ for some $i \in \mathcal{N}$, where $G_{ii} \in \mathbb{R}_{>0}$ is the shunt conductance and $\hat{B}_{ii} \in \mathbb{R}_{<0}$ denotes the inductive shunt susceptance. For convenience, we define $\hat{Y}_{ii} := 0$ whenever there is no shunt admittance present at a node $i \in \mathcal{N}$. Finally, we assume that the loading in the original network is such that no power or

---

[1]To the best of our knowledge, there does not exist one standard load model. The main reason for this is that there are typically many different kinds of loads connected within one power system or microgrid, see, e.g., [10], [38], [39]. Therefore, we are aware that not all loads can be accurately represented by constant impedance loads and our results may be inaccurate for other type of load models, such as dynamic loads [39].

voltage constraints are violated at any time.

The overall active and reactive power flows $P_i : \mathbb{T}^n \times \mathbb{R}_{>0}^n \to \mathbb{R}$ and $Q_i : \mathbb{T}^n \times \mathbb{R}_{>0}^n \to \mathbb{R}$ at a node $i \in \mathcal{N}$ are obtained as[2]

$$
\begin{aligned}
P_i(\delta_1, \ldots, \delta_n, V_1, \ldots, V_n) = \\
G_{ii}V_i^2 + \sum_{k \sim \mathcal{N}_i} |B_{ik}|V_i V_k \sin(\delta_{ik}), \\
Q_i(\delta_1, \ldots, \delta_n, V_1, \ldots, V_n) = \\
|B_{ii}|V_i^2 - \sum_{k \sim \mathcal{N}_i} |B_{ik}|V_i V_k \cos(\delta_{ik}),
\end{aligned}
\tag{1}
$$

with $B_{ii} := \hat{B}_{ii} + \sum_{k \sim \mathcal{N}_i} B_{ik}$. Hence,

$$
|B_{ii}| \geq \sum_{k \sim \mathcal{N}_i} |B_{ik}|.
\tag{2}
$$

To motivate the voltage control proposed in Section III and to establish the results in Sections IV and V, we make use of the standard decoupling assumption[3], see [10], [18].

Assumption II.2. $\delta_{ik}(t) \approx 0 \quad \forall t \geq 0, \ i \sim \mathcal{N}, \ k \sim \mathcal{N}_i.$

Under Assumption II.2, $\cos(\delta_{ik}(t)) \approx 1$, for all $t \geq 0$ and $i \sim \mathcal{N}$, $k \sim \mathcal{N}_i$. Consequently, the reactive power flow at a node $i \in \mathcal{N}$ reduces to $Q_i : \mathbb{R}_{>0}^n \to \mathbb{R}$

$$
Q_i(V_1, \ldots, V_n) = |B_{ii}|V_i^2 - \sum_{k \sim \mathcal{N}_i} |B_{ik}|V_i V_k.
\tag{3}
$$

Clearly, the reactive power Q_i can then be controlled by controlling the voltage amplitudes V_i and V_k, $k \in \mathcal{N}_i$. This fact is used when designing a distributed voltage control for reactive power sharing in Section III.

The apparent power flow is given by $S_i = P_i + jQ_i$. Since we are mainly concerned with dynamics of generation units, we express all power flows in generator convention [40]. That is, delivered active power is positive, while absorbed active power is negative; capacitive reactive power is counted positively and inductive reactive power is counted negatively.

Remark II.3. *The restriction to inductive shunt admittances is justified as follows. The admittance loads in the Kron-reduced network are a conglomeration of the individual loads in the original network, see, e.g., [10], [41]. Therefore, assuming purely inductive loads in the Kron-reduced network can be interpreted as assuming that the original network is not overcompensated, i.e., that the overall load possesses inductive character. Furthermore, capacitive shunt admittances in distribution systems mainly stem from capacitor banks used to compensate possibly strong inductive behaviors of loads. In conventional distribution systems, these devices are additionally inserted in the system to improve its performance with respect to reactive power consumption [10], [23]. This is needed because there is no generation located close to the loads. However, in a microgrid, the generation units are located close to the loads. Hence, the availability of generation*

units at distribution level is likely to replace the need for capacitor banks, see also [23].

B. Inverter model

We model the inverters as AC voltage sources the amplitude and frequency of which can be defined by the designer [5], [6], [8].[4] Then, an inverter at node $i \in \mathcal{N}$ can be represented as [6], [13]

$$
\begin{aligned}
\dot{\delta}_i &= u_i^\delta, \\
\tau_{P_i} \dot{P}_i^m &= -P_i^m + P_i, \\
V_i &= u_i^V, \\
\tau_{P_i} \dot{Q}_i^m &= -Q_i^m + Q_i,
\end{aligned}
\tag{4}
$$

where $u_i^\delta : \mathbb{R}_{\geq 0} \to \mathbb{R}$ and $u_i^V : \mathbb{R}_{\geq 0} \to \mathbb{R}$ are controls. Furthermore, it is assumed that the active and reactive power outputs P_i and Q_i given in (1) are measured and processed through a filter with time constant $\tau_{P_i} \in \mathbb{R}_{>0}$ [11], [42]. We furthermore associate to each inverter its power rating $S_i^N \in \mathbb{R}_{>0}$, $i \sim \mathcal{N}$.

C. Communication network

The proposed voltage control is distributed and requires communication among generation units in the network. To describe the high-level properties of the communication network, a graph theoretic notation is used in the paper.

We assume that the communication network is represented by an undirected and connected graph $\mathcal{G} = (\mathcal{V}, \mathcal{E})$. Furthermore, we assume that the graph contains no self-loops, i.e., there is no edge $e_l = \{i, i\}$. A node represents an individual agent. In the present case, this is a power generation source. If there is an edge between two nodes i and k, then i and k can exchange their local measurements with each other. The nodes in the communication and in the electrical network are identical, i.e., $\mathcal{N} \equiv \mathcal{V}$. Note that the communication topology may, but does not necessarily have to, coincide with the topology of the electrical network, i.e., we may allow $\mathcal{C}_i \neq \mathcal{N}_i$ for any $i \in \mathcal{V}$.

III. POWER SHARING AND INVERTER CONTROL

In this section the frequency and voltage controls u_i^δ and u_i^V for the inverters represented by (4) are introduced. Recall that power sharing is an important performance criterion in microgrids. The concept of proportional power sharing is formalized via the following definition.

Definition III.1. *Let $\gamma_i \in \mathbb{R}_{>0}$ and $\chi_i \in \mathbb{R}_{>0}$ denote constant weighting factors and P_i^s, respectively Q_i^s, the steady-state active, respectively reactive, power flow, $i \sim \mathcal{N}$. Then, two inverters at nodes i and k are said to share their active,*

---

[2]To simplify notation the time argument of all signals is omitted from now on.

[3]Our results in Sections IV and V also hold for arbitrary, but constant angle differences, i.e., $\delta_{ik}(t) := \delta_{ik}$, $\delta_{ik} \in \mathbb{T}$, but at the cost of a more complex notation.

[4]An underlying assumption to this model is that whenever the inverter connects an intermittent renewable generation source, e.g., a photovoltaic plant or a wind plant, to the network, it is equipped with some sort of storage (e.g., flywheel, battery). Thus, it can increase and decrease its power output within a certain range.

respectively reactive, powers proportionally according to γ_i and γ_k, respectively χ_i and χ_k, if

$$\frac{P_i^s}{\gamma_i} = \frac{P_k^s}{\gamma_k}, \quad \text{respectively} \quad \frac{Q_i^s}{\chi_i} = \frac{Q_k^s}{\chi_k}.$$

Remark III.2. *From* (4) *it follows that in steady-state* $\dot{P}_i^m = 0$ *and* $\dot{Q}_i^m = 0$. *Hence,* $P_i^{m,s} = P_i^s$ *and* $Q_i^{m,s} = Q_i^s$, *where the superscript* s *denotes signals in steady-state.*

Remark III.3. *A practical choice for* γ_i *and* χ_i *would, for example, be* $\gamma_i = \chi_i = S_i^N$, *where* $S_i^N \in \mathbb{R}_{>0}$ *is the nominal power rating of the inverter at node* $i \in \mathcal{N}$. *However, an operator may also wish to consider other technical, economic or environmental criteria, such as fuel consumption, generation costs or emission costs, when determining the weighting coefficients* γ_i *and* χ_i, $i \sim \mathcal{N}$, *see, e.g.,* [43], [44].

A. Frequency droop control and active power sharing

For the problem of active power sharing, the following decentralized proportional control law, commonly referred to as **frequency droop control** [9], is often employed

$$u_i^\delta = \omega^d - k_{P_i}(P_i^m - P_i^d), \tag{5}$$

where $\omega^d \in \mathbb{R}_{>0}$ is the desired (nominal) frequency, $k_{P_i} \in \mathbb{R}_{>0}$ the frequency droop gain, P_i^m the measured active power and $P_i^d \in \mathbb{R}$ its desired setpoint.

It is shown in [12]–[14] that the following selection of control gains and setpoints for the control law (5) guarantees a proportional active power distribution in steady-state in the sense of Definition III.1

$$k_{P_i}\gamma_i = k_{P_k}\gamma_k, \quad k_{P_i}P_i^d = k_{P_k}P_k^d. \tag{6}$$

A detailed physical motivation for the control law (5) is given in [13].

B. Distributed voltage control (DVC)

Following the heuristics of the frequency droop control (5), droop control is typically also applied with the goal to achieve a desired reactive power distribution in microgrids. The most common (heuristic) **voltage droop control** is given by [1], [9]

$$u_i^V = V_i^d - k_{Q_i}(Q_i^m - Q_i^d), \tag{7}$$

where $V^d \in \mathbb{R}_{>0}$ is the desired (nominal) voltage, $k_{Q_i} \in \mathbb{R}_{>0}$ the voltage droop gain, Q_i^m the measured reactive power and $Q_i^d \in \mathbb{R}$ its desired setpoint. The control law (7) is decentralized, i.e., the feedback signal is the locally measured reactive power Q_i^m, and it does therefore not require communication. However, to the best of the authors' knowledge, there are no known selection criteria for the parameters of the voltage droop control (7) that would ensure a desired reactive power sharing, see also [13], [17], [18].

Inspired by consensus-algorithms, see e.g., [28], we therefore propose the following **distributed voltage control (DVC)**
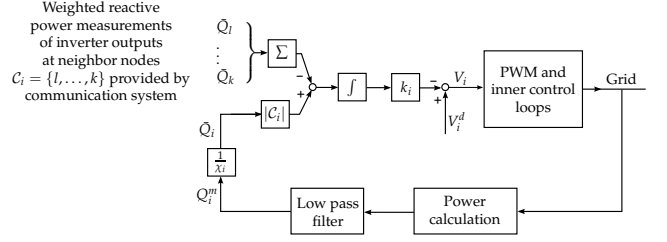

Fig. 1: Block diagram of the proposed DVC for an inverter at node $i \in \mathcal{N}$. V_i is the voltage amplitude, V_i^d its desired (nominal) value, Q_i^m is the measured reactive power and $\bar{Q}_i$ the weighted reactive power, where χ_i is the weighting coefficient to ensure proportional reactive power sharing and k_i is a feedback gain.

u_i^V for an inverter at node $i \in \mathcal{N}$

$$u_i^V(t) := V_i^d - k_i \int_0^t e_i(\tau)d\tau,$$

$$e_i(t) := \sum_{k \sim \mathcal{C}_i} \left(\frac{Q_i^m(t)}{\chi_i} - \frac{Q_k^m(t)}{\chi_k} \right) = \sum_{k \sim \mathcal{C}_i} (\bar{Q}_i(t) - \bar{Q}_k(t)), \tag{8}$$

where $V_i^d \in \mathbb{R}_{>0}$ is the desired (nominal) voltage amplitude and $k_i \in \mathbb{R}_{>0}$ is a feedback gain. For convenience, we have defined the weighted reactive power flows $\bar{Q}_i := Q_i^m/\chi_i$, $i \sim \mathcal{N}$. Recall that $\mathcal{C}_i$ defined in II-C is the set of neighbor nodes of node i in the graph induced by the communication network, i.e., the set of nodes that node i can exchange information with. The control scheme is illustrated for an inverter at node $i \in \mathcal{N}$ in Fig. 1. We prove in Section V that the control (8) does guarantee proportional reactive power sharing in steady-state.

Remark III.4. *Consider a scenario in which there exists a high-level control that can generate setpoints* Q_i^d, $i \sim \mathcal{N}$, *for the reactive power injections. A possible high-level control is, for example, the one proposed in* [25]. *The control* (8) *can easily be combined with such high-level control by setting* e_i *given in* (8) *to*

$$e_i = \sum_{k \sim \mathcal{C}_i} \left(\frac{(Q_i^m - Q_i^d)}{\chi_i} - \frac{(Q_k^m - Q_k^d)}{\chi_k} \right). \tag{9}$$

Then the inverters share their absolute reactive power injections with respect to individual setpoints in steady-state.

Remark III.5. *In addition to reactive power sharing, it usually is desired that the voltage amplitudes* V_i, $i \sim \mathcal{N}$, *remain within certain bounds. With the control law* (8), *where the voltage amplitudes are actuator signals, this can, e.g., be ensured by saturating the control signal* u_i^V. *In that case, the performance in reactive power sharing could be degradaded when the control signal is saturated. For mathematical simplicity, this is not considered in the present analysis.*

C. Closed-loop voltage and reactive power dynamics

To establish the results in Sections IV and V, we make use of the standard decoupling Assumption II.2. It follows from (3) that the influence of the dynamics of the phase angles on the

reactive power flows can then be neglected. Since, moreover, the DVC given in (8) only uses reactive power measurements, the model (4) can be reduced to

$$V_i = u_i^v,$$
$$\tau \dot{Q}_i^m = -Q_i^m + Q_i. \tag{10}$$

Differentiating $V_i = u_i^V$ with respect to time and combining (8) and (10), the closed-loop dynamics of the i-th node are given by

$$\dot{V}_i = -k_i e_i = -k_i \sum_{k \sim \mathcal{C}_i} \left(\frac{Q_i^m}{\chi_i} - \frac{Q_k^m}{\chi_k} \right),$$
$$\tau_{P_i} \dot{Q}_i^m = -Q_i^m + Q_i, \tag{11}$$

and the interaction between nodes is modeled by (3). Note that $V_i(0) = V_i^d$ is determined by the control law (8).

Recalling from II-C that $\mathcal{L} \in \mathbb{R}^{n \times n}$ is the Laplacian matrix of the communication network and defining the $n \times n$ matrices

$$T := \text{diag}(\tau_{P_i}), D := \text{diag}(1/\chi_i), K := \text{diag}(k_i),$$

as well as the column vectors $V \in \mathbb{R}^n, Q \in \mathbb{R}^n$ and $Q^m \in \mathbb{R}^n$

$$V := \text{col}(V_i), \quad Q := \text{col}(Q_i), \quad Q^m := \text{col}(Q_i^m),$$

the **closed-loop system** dynamics can be written compactly in matrix form as

$$\dot{V} = -K\mathcal{L}DQ^m,$$
$$T\dot{Q}^m = -Q^m + Q, \tag{12}$$

where $Q_i = Q_i(V)$ is given by (3) and the initial conditions for each element of V are determined by the control law (8), i.e., $V(0) = V^d := \text{col}(V_i^d), i \sim \mathcal{N}$.

Remark III.6. *Recall that an inverter represented by (4) is operated in grid-forming mode, which implies that the amplitude and frequency of the voltage provided at the inverter terminals can be specified by the operator, respectively, by a suitable control [8]. This also applies to the initial conditions of the voltages $V(0) = V^d$ in (12).*

D. Reactive power sharing and a voltage conservation law

The next result proves that the proposed DVC does indeed guarantee proportional reactive power sharing in steady-state.

Claim III.7. *The control law (8) achieves proportional reactive power sharing in steady-state in the sense of Definition III.1.*

Proof. Set $\dot{V} = 0$ in (12). Note that, since $\mathcal{L}$ is the Laplacian matrix of an undirected connected graph, it has a simple zero eigenvalue with a corresponding right eigenvector $\beta \underline{1}_n, \beta \in \mathbb{R} \setminus \{0\}$. All its other eigenvalues are positive real. Moreover, K is a diagonal matrix with positive diagonal entries and from (12) in steady-state $Q^s = Q^{m,s}$. Hence, for $\beta \in \mathbb{R} \setminus \{0\}$ and $i \sim \mathcal{N}, k \sim \mathcal{N}$

$$\underline{0}_n = -K\mathcal{L}DQ^s \Leftrightarrow DQ^s = \beta \underline{1}_n \Leftrightarrow \frac{Q_i^s}{\chi_i} = \frac{Q_k^s}{\chi_k}. \tag{13}$$

□□□

Remark III.8. *Because of (13), all entries of $Q^{m,s} = Q^s(V^s)$ must have the same sign. Since we consider inductive networks and loads, only $Q^{m,s} = Q^s(V^s) \in \mathbb{R}_{>0}^n$ is practically relevant.*

The following fact reveals an important property of the system (12), (3).

Fact III.9. *The flow of the system (12), (3) satisfies for all $t \geq 0$ the conservation law*

$$\|K^{-1}V(t)\|_1 = \sum_{i=1}^n \frac{V_i(t)}{k_i} = \xi(V(0)), \tag{14}$$

where the positive real parameter $\xi(V(0))$ is given by

$$\xi(V(0)) = \|K^{-1}V(0)\|_1 = \sum_{i=1}^n \frac{V_i^d}{k_i}. \tag{15}$$

Proof. Recall that $\mathcal{L}$ is the Laplacian matrix of an undirected connected graph. Consequently, $\mathcal{L}$ is symmetric positive semidefinite and possesses a simple zero eigenvalue with corresponding right eigenvector $\underline{1}_n$, i.e., $\mathcal{L} = \mathcal{L}^T$ and $\mathcal{L}\underline{1}_n = \underline{0}_n$. Hence, $\underline{1}_n^T \mathcal{L} = \underline{0}_n^T$. Multiplying the first equation in (12) from the left with $\underline{1}_n^T K^{-1}$ yields

$$\underline{1}_n^T K^{-1}\dot{V} = \underline{0}_n^T DQ^m \quad \Rightarrow \quad \sum_{i=1}^n \frac{\dot{V}_i}{k_i} = 0. \tag{16}$$

Integrating (16) with respect to time and using (15) yields (14). □□□

Fact III.9 has the following important practical implication: by interpreting the control gains k_i as weighting coefficients, expression (14) is equivalent to the weighted average voltage amplitude $\bar{V}(t)$ in the network, i.e.,

$$\bar{V}(t) := \frac{1}{n}\sum_{i=1}^n \frac{V_i(t)}{k_i}.$$

By Fact III.9, we then have that for all $t \geq 0$

$$\bar{V}(t) := \bar{V}(0) = \frac{\xi(V(0))}{n} = \frac{1}{n}\sum_{i=1}^n \frac{V_i^d}{k_i}. \tag{17}$$

Hence, the parameters V_i^d and k_i, $i \sim \mathcal{N}$, offer useful degrees of freedom for a practical implementation of the DVC (8). For example, a typical choice for V_i^d would be $V_i^d = V_N$, $i \sim \mathcal{N}$, where V_N denotes the nominal voltage amplitude. By setting $k_i = 1$, $i \sim \mathcal{N}$, (17) becomes

$$\bar{V}(t) := \frac{1}{n}\sum_{i=1}^n V_i(t) = V_N, \tag{18}$$

i.e., the average voltage amplitude $\bar{V}(t)$ of all generator buses in the network is for all $t \geq 0$ equivalent to the nominal voltage amplitude V_N.

Remark III.10. *Note that achieving (18) for $t \to \infty$ is exactly the control goal of the distributed voltage control proposed in [34], Section IV-B. As we have just shown, for $V_i^d = V_N$, $k_i = 1, i \sim \mathcal{N}$, the DVC (8) not only guarantees compliance of (18) for $t \to \infty$, but for all $t \geq 0$. In addition, by Claim III.7,*

the DVC (8) *guarantees a desired reactive power sharing in steady-state.*

Remark III.11. *Let* $x^s = col(V^s, Q^s)$ *be an equilibrium point of the system* (12), (3). *It follows from Fact III.9 that only solutions of the system* (12), (3) *with initial conditions satisfying*

$$\|K^{-1}V(0)\|_1 = \|K^{-1}V^s\|_1$$

can converge to x^s.

IV. EXISTENCE AND UNIQUENESS OF EQUILIBRIA

To streamline the presentation of the main result within this section, it is convenient to introduce the matrix $\mathcal{T} \in \mathbb{R}^{n \times n}$ with entries

$$\mathcal{T}_{ii} := |B_{ii}|, \quad \mathcal{T}_{ik} := -|B_{ik}|, \quad i \neq k. \tag{19}$$

Lemma IV.1. *The matrix* $\mathcal{T}$ *is positive definite.*

Proof. Recall that $B_{ii} = \hat{B}_{ii} + \sum_{k \sim \mathcal{N}_i} B_{ik}$ and (2). It is then easily verified that the matrix

$$\mathcal{T} - \mathrm{diag}(|\hat{B}_{ii}|),$$

is a symmetric weighted Laplacian matrix. Recall that the microgrid is connected by assumption. Consequently, $\mathcal{T} - \mathrm{diag}(|\hat{B}_{ii}|)$ possesses a simple zero eigenvalue with a corresponding right eigenvector $\underline{1}_n$ and all its other eigenvalues are positive real, i.e., for any $v \in \mathbb{R}^n \setminus \{\beta \underline{1}_n\}$, $\beta \in \mathbb{R} \setminus \{0\}$

$$\left(\mathcal{T} - \mathrm{diag}(|\hat{B}_{ii}|)\right)\underline{1}_n = \underline{0}_n, \; v^T\left(\mathcal{T} - \mathrm{diag}(|\hat{B}_{ii}|)\right)v \in \mathbb{R}_{>0}.$$

Furthermore, recall that $\hat{B}_{ii} \neq 0$ for at least some $i \in \mathcal{N}$. Hence, $\mathcal{T}$ is positive definite. □□□

The proposition below proves existence of equilibria of the system (12), (3). In addition, it shows that the control parameters uniquely determine the corresponding equilibrium point of the system (12), (3). We demonstrate in the simulation study in Section VI that the tuning parameter κ (introduced in the proposition) allows to easily shape the performance of the closed-loop dynamics.

Proposition IV.2. *Consider the system* (12), (3). *Fix D and a positive real constant α. Set $K = \kappa \mathcal{K}$, where κ is a positive real parameter and $\mathcal{K} \in \mathbb{R}^{n \times n}$ a diagonal matrix with positive real diagonal entries. To all initial conditions $col(V(0), Q^m(0))$ with the property*

$$\|\mathcal{K}^{-1}V(0)\|_1 = \alpha, \tag{20}$$

there exists a unique positive equilibrium point $col(V^s, Q^{m,s}) \in \mathbb{R}_{>0}^{2n}$. Moreover, to any α there exists a unique positive constant β such that

$$\|\mathcal{K}^{-1}V^s\|_1 = \alpha, \quad Q^s = Q^{m,s} = \beta D^{-1}\underline{1}_n. \tag{21}$$

Proof. To establish the claim, we first prove that to each $Q^s \in \mathbb{R}_{>0}^n$ satisfying (21) there exists a unique $V^s \in \mathbb{R}_{>0}^n$. To this end, consider (13). Clearly, any $Q^s = \beta D^{-1}\underline{1}_n$, $\beta \in \mathbb{R}_{>0}$

satisfies (13) and is hence a possible vector of positive steady-state reactive power flows. Fix a $\beta \in \mathbb{R}_{>0}$. Because of

$$Q_i^s = |B_{ii}|V_i^{s^2} - \sum_{k \sim \mathcal{N}_i} |B_{ik}|V_i^s V_k^s, \quad i \sim \mathcal{N}, \tag{22}$$

no element V_i^s can then be zero. Hence, (22) can be rewritten as

$$-\frac{Q_i^s}{V_i^s} + |B_{ii}|V_i^s - \sum_{k \sim \mathcal{N}_i} |B_{ik}|V_k^s = 0, \quad i \sim \mathcal{N},$$

or, more compactly,

$$F(V^s) + \mathcal{T}V^s = \underline{0}_n, \tag{23}$$

where $F(V^s) := col(-Q_i^s/V_i^s) \in \mathbb{R}^n$ and $\mathcal{T}$ is defined in (19). Recall that according to Lemma IV.1, $\mathcal{T}$ is positive definite. Consider the function $f : \mathbb{R}_{>0}^n \to \mathbb{R}$,

$$f(V) := \frac{1}{2}V^T\mathcal{T}V - \sum_{i=1}^n Q_i^s \ln(V_i),$$

which has the property that

$$\left(\frac{\partial f(V)}{\partial V}\right)^T = F(V) + \mathcal{T}V.$$

Hence, any critical point of f satisfies (23), respectively (22). Moreover,

$$\frac{\partial^2 f(V)}{\partial V^2} = \mathrm{diag}\left(\frac{Q_i^s}{V_i^2}\right) + \mathcal{T} > 0,$$

which means that the Hessian of f is positive definite for all $V \in \mathbb{R}_{>0}^n$. Therefore, f is a strictly convex continuous function on the convex set $\mathbb{R}_{>0}^n$. Note that f tends to infinity on the boundary of $\mathbb{R}_{>0}^n$, i.e.,

$$f(V) \to \infty \quad \text{as} \quad \|V\|_\infty \to \infty,$$
$$f(V) \to \infty \quad \text{as} \quad \min_{i \in \mathcal{N}}(V_i) \to 0.$$

Hence, there exist positive real constants $m_0 \gg 1$, $r_1 \ll 1$ and $r_2 \gg 1$, such that

$$\mathcal{W} := \{V \in \mathbb{R}_{>0}^n \mid \min_{i \in \mathcal{N}}(V_i) \geq r_1 \wedge \|V\|_\infty \leq r_2\},$$

$$V \in \mathbb{R}_{>0}^n \setminus \mathcal{W} \quad \Rightarrow \quad f(V) > m_0,$$

$$\exists V \in \mathcal{W} \quad \text{such that} \quad f(V) < m_0.$$

Clearly, $\mathcal{W}$ is a compact set. Hence, by the Weierstrass extreme value theorem [45], f attains a minimum on $\mathcal{W}$. By construction, this minimum is attained at the interior of $\mathcal{W}$, which by differentiability of f implies that it is a critical point of f. Consequently, the vector $V^s := \arg\min_{V \in \mathcal{W}}(f(V))$ is the unique solution of (23) and thus the unique positive vector of steady-state voltage amplitudes corresponding to a given positive vector of steady-state reactive power flows Q^s. This proves existence of equilibria of the system (12), (3). Moreover, it shows that to a given $Q^s \in \mathbb{R}_{>0}^n$, there exists a unique corresponding $V^s \in \mathbb{R}_{>0}^n$.

We next prove by contradiction that the constant α uniquely determines the positive equilibrium point $col(V^s, Q^s) \in \mathbb{R}_{>0}^{2n}$ corresponding to all initial conditions $col(V(0), Q^m(0))$ with

the property (20). Assume that there exist two different positive equilibrium points $\mathrm{col}(V_1^s, Q_1^s) \in \mathbb{R}_{>0}^{2n}$ and $\mathrm{col}(V_2^s, Q_2^s) \in \mathbb{R}_{>0}^{2n}$ with the following property

$$\|\mathcal{K}^{-1}V_1^s\|_1 = \|\mathcal{K}^{-1}V_2^s\|_1 = \alpha. \tag{24}$$

It follows from (13) that the vectors Q_1^s and Q_2^s are identical up to multiplication by a positive real constant ϑ, i.e.,

$$Q_2^s = \vartheta Q_1^s.$$

The uniqueness result above implies $\vartheta \neq 1$, i.e., $Q_1^s \neq Q_2^s$. Otherwise V_1^s and V_2^s would coincide and the two equilibrium points would be the same. Clearly, if $\mathrm{col}(V_1^s, Q_1^s)$ satisfies (22), then $\mathrm{col}(V_2^s, Q_2^s) = \mathrm{col}(\sqrt{\vartheta}V_1^s, \vartheta Q_1^s)$, $\vartheta > 0$, also satisfies (22) and, because of the uniqueness result, $V_2^s = \sqrt{\vartheta}V_1^s$ is the unique steady-state voltage vector corresponding to Q_2^s. As $\vartheta \neq 1$, it follows immediately that (24) is violated. The proof is completed by recalling that Fact III.9 implies that

$$\|\mathcal{K}^{-1}V(t)\|_1 = \|\mathcal{K}^{-1}V(0)\|_1$$

for all $t \geq 0$. □□□

Remark IV.3. *The following useful property is an immediate consequence of Proposition IV.2. Suppose $\mathrm{col}(V^s, Q^{m,s}) \in \mathbb{R}_{>0}^{2n}$ is a known equilibrium point of the system (12), (3) with the properties $Q^s = \beta D^{-1}\mathbb{1}_n$ and $\|\mathcal{K}^{-1}V^s\|_1 = \alpha$. Then for any $\vartheta \in \mathbb{R}_{>0}$ and for all initial conditions $\mathrm{col}(V(0), Q^m(0))$ with the property $\|\mathcal{K}^{-1}V(0)\|_1 = \sqrt{\vartheta}\alpha$, the corresponding unique equilibrium point is given by $\mathrm{col}(\sqrt{\vartheta}V^s, \vartheta Q^{m,s})$.*

Remark IV.4. *Fix a real constant α. Consider a linear first-order consensus system with state vector $x \in \mathbb{R}^n$ and dynamics $\dot{x} = -\mathcal{L}x$, $x(0) = x_0$, where $\mathcal{L} \in \mathbb{R}^{n \times n}$ is the Laplacian matrix of the communication network. It is well-known, see e.g., [28], that if the graph model of the communication network is undirected and connected, then*

$$x^s = \frac{1}{n}\mathbb{1}_n^T x_0 \mathbb{1}_n = \frac{1}{n}\left(\sum_{i=1}^n x_i(0)\right)\mathbb{1}_n.$$

Hence, to all x_0 with the property $\sum_{i=1}^n x_i(0) = \alpha$, there exists a unique x^s with $\sum_{i=1}^n x_i^s = \alpha$. Proposition IV.2 shows that the nonlinear system (12), (3) exhibits an equivalent property.

V. STABILITY

In this section we establish necessary and sufficient conditions for local exponential stability of equilibria of the system (12), (3). To this end, we make the following important observation. It follows from Fact III.9 that the motion of an arbitrary voltage V_i, $i \in \mathcal{N}$, can be expressed in terms of all other voltages V_k, $k \sim \mathcal{N} \setminus \{i\}$ for all $t \geq 0$. This implies that studying the stability properties of equilibra of the system (12), (3) with dimension $2n$, is equivalent to studying the stability properties of corresponding equilibria of a reduced system of dimension $2n - 1$.

For ease of notation and without loss of generality, we choose to express V_n as

$$V_n = k_n\xi(V(0)) - \sum_{i=1}^{n-1}\frac{k_n}{k_i}V_i, \tag{25}$$

with $\xi(V(0))$ given by (15). Furthermore, we define the reduced voltage vector $V_R \in \mathbb{R}_{>0}^{n-1}$ as

$$V_R := \mathrm{col}(V_1, \ldots V_{n-1}), \tag{26}$$

and denote the reactive power flows in the new coordinates by

$$Q_{R_i}(V_1, \ldots, V_{n-1}) = |B_{ii}|V_i^2 - \sum_{k \sim \mathcal{N}_i}|B_{ik}|V_iV_k,$$
$$Q_{R_n}(V_1, \ldots, V_{n-1}) = |B_{nn}|V_n^2 - \sum_{k \sim \mathcal{N}_n}|B_{nk}|V_kV_n, \tag{27}$$

where $V_n = V_n(V_1, \ldots, V_{n-1})$ and $i \sim \mathcal{N} \setminus \{n\}$. By defining the matrix $\mathcal{L}_R \in \mathbb{R}^{(n-1) \times n}$

$$\mathcal{L}_R := \begin{bmatrix} I_{n-1} & 0_{n-1} \end{bmatrix}K\mathcal{L}, \tag{28}$$

the system (12), (3) can be written in the reduced coordinates $\mathrm{col}(V_R, Q^m) \in \mathbb{R}_{>0}^{n-1} \times \mathbb{R}^n$ as

$$\dot{V}_R = -\mathcal{L}_R DQ^m,$$
$$T\dot{Q}^m = -Q^m + Q_R, \tag{29}$$

with $Q_R := \mathrm{col}(Q_{R_i}) \in \mathbb{R}^n$ and Q_{R_i}, $i \sim \mathcal{N}$, given in (27).

A. Error states and linearization

Recall Proposition IV.2. Clearly, the existence and uniqueness properties of the system (12), (3) hold equivalently for the reduced system (29), (27) with V_n given in (25). Let $\mathrm{col}(V^s, Q^{m,s}) \in \mathbb{R}_{>0}^{2n}$ be a positive equilibrium point of the system (12), (3) and $\mathrm{col}(V_R^s, Q^{m,s}) \in \mathbb{R}_{>0}^{2n-1}$ be the corresponding equilibrium point of the system (29), (27). It follows from (25) that

$$\frac{\partial V_n(V_1, \ldots, V_{n-1})}{\partial V_i} = -\frac{k_n}{k_i}, \quad i \sim \mathcal{N} \setminus \{n\}.$$

Consequently, the partial derivative of the reactive power flow Q_{R_k}, $k \sim \mathcal{N}$, given in (29), (27) with respect to the voltage V_i, $i \sim \mathcal{N} \setminus \{n\}$, can be written as

$$\frac{\partial Q_{R_k}}{\partial V_i} = \frac{\partial Q_k}{\partial V_i} - \frac{k_n}{k_i}\frac{\partial Q_k}{\partial V_n}, \quad i \sim \mathcal{N} \setminus \{n\}. \tag{30}$$

Hence, by introducing the matrix

$$N := \frac{\partial Q}{\partial V}\Big|_{V^s} \in \mathbb{R}^{n \times n}$$

with entries (use (3))

$$n_{ii} := 2|B_{ii}|V_i^s - \sum_{k \sim \mathcal{N}_i}|B_{ik}|V_k^s, \quad n_{ik} := -|B_{ik}|V_i^s, \quad i \neq k, \tag{31}$$

as well as the matrix $\mathcal{R} \in \mathbb{R}^{n \times (n-1)}$

$$\mathcal{R} := \begin{bmatrix} I_{(n-1)} \\ -b^T \end{bmatrix}, \quad b := \mathrm{col}\left(\frac{k_n}{k_1}, \ldots, \frac{k_n}{k_{n-1}}\right), \tag{32}$$

and by making use of (30), it follows that

$$\frac{\partial Q_R}{\partial V_R}\Big|_{V_R^s} = N\mathcal{R}. \tag{33}$$

To derive an analytic stability condition it is convenient to assume identical low pass filter time constants.

Assumption V.1. *The time constants of the low pass filters in (12) are chosen such that $\tau = \tau_{P_1} = \ldots = \tau_{P_n}$.*

Remark V.2. *In practice, the low-pass filters are typically implemented in order to filter the fundamental component of the power injections [11]. Hence, Assumption V.1 is not overly conservative in practice.*

Furthermore, we define the deviations of the system variables with respect to the given equilibrium point $\mathrm{col}(V_R^s, Q^{m,s}) \in \mathbb{R}_{>0}^{2n-1}$ as

$$\tilde{V}_R := V_R - V_R^s \in \mathbb{R}^{n-1},$$
$$\tilde{Q}^m := Q^m - Q^{m,s} \in \mathbb{R}^n.$$

Linearizing the microgrid (29), (27) at this equilibrium point and making use of (33) together with Assumption V.1 yields

$$\begin{bmatrix} \dot{\tilde{V}}_R \\ \dot{\tilde{Q}}^m \end{bmatrix} = \underbrace{\begin{bmatrix} 0_{(n-1)\times(n-1)} & -\mathcal{L}_R D \\ \frac{1}{\tau} N\mathcal{R} & -\frac{1}{\tau} I_n \end{bmatrix}}_{:=A} \begin{bmatrix} \tilde{V}_R \\ \tilde{Q}^m \end{bmatrix}. \tag{34}$$

Note that

$$\mathcal{R}\mathcal{L}_R = \mathcal{R} \begin{bmatrix} I_{n-1} & 0_{n-1} \end{bmatrix} K\mathcal{L} = \begin{bmatrix} I_{n-1} & 0_{n-1} \\ -b^T & 0 \end{bmatrix} K\mathcal{L}$$
$$= K \begin{bmatrix} I_{n-1} & 0_{n-1} \\ -1_{n-1}^T & 0 \end{bmatrix} \mathcal{L} = K\mathcal{L}, \tag{35}$$

and that

$$\mathcal{R}^T K^{-1} 1_n = 0_{n-1}. \tag{36}$$

B. Condition for local exponential stability

The main contribution of this section is to give a necessary and sufficient condition for local exponential stability of an equilibrium point of the system (29), (27).

Lemma V.3. *For $Q^s, V^s \in \mathbb{R}_{>0}^n$, all eigenvalues of N have positive real part.*

Proof. Dividing (22) by $V_i^s > 0$ yields

$$\frac{Q_i^s}{V_i^s} = |B_{ii}|V_i^s - \sum_{k \sim \mathcal{N}_i} |B_{ik}|V_k^s > 0. \tag{37}$$

Furthermore, from (2) it follows that

$$|B_{ii}|V_i^s \geq \sum_{k \sim \mathcal{N}_i} |B_{ik}|V_i^s. \tag{38}$$

Hence, with n_{ii} and n_{ik} defined in (31) we have that

$$n_{ii} = 2|B_{ii}|V_i^s - \sum_{k \sim \mathcal{N}_i} |B_{ik}|V_k^s > |B_{ii}|V_i^s \geq \sum_{k \sim \mathcal{N}\backslash\{i\}} |n_{ik}|.$$

Therefore, N is a diagonally dominant matrix with positive diagonal elements and the claim follows from Gershgorin's disc theorem [46]. □□□

Lemma V.4. *For $Q^s, V^s \in \mathbb{R}_{>0}^n$, the matrix product $ND\mathcal{L}D$ has a zero eigenvalue with geometric multiplicity one and a corresponding right eigenvector $\beta D^{-1} 1_n$, $\beta \in \mathbb{R} \setminus \{0\}$; all other eigenvalues have positive real part.*

Proof. The matrix D is diagonal with positive diagonal entries and hence positive definite. Furthermore, $\mathcal{L}$ is the Laplacian matrix of an undirected connected graph and therefore positive semidefinite. We also know that $\mathcal{L}$ has a simple zero eigenvalue

with a corresponding right eigenvector $\beta 1_n$, $\beta \in \mathbb{R} \setminus \{0\}$. Moreover, Lemma V.3 implies that N is nonsingular. Consequently,

$$ND\mathcal{L}Dv = 0_n \Leftrightarrow \mathcal{L}Dv = 0_n \Leftrightarrow v = \beta D^{-1} 1_n, \beta \in \mathbb{R}\backslash\{0\}.$$

Hence, $ND\mathcal{L}D$ has a zero eigenvalue with geometric multiplicity one and a corresponding right eigenvector $\beta D^{-1} 1_n$, $\beta \in \mathbb{R} \setminus \{0\}$. In addition, $D\mathcal{L}D$ is positive semidefinite and by Lemma II.1 it follows that

$$\sigma(ND\mathcal{L}D) \subseteq W(N)W(D\mathcal{L}D).$$

By the aforementioned properties of D and $\mathcal{L}$, we have that $W(D\mathcal{L}D) \subseteq \mathbb{R}_{\geq 0}$. To prove that all eigenvalues apart from the zero eigenvalue have positive real part, we show that $\Re(W(N)) \subseteq \mathbb{R}_{>0}$. This also implies that the only element of the imaginary axis in $W(N)W(D\mathcal{L}D)$ is the origin. To see this, we recall that the real part of the numerical range of N is given by the range of its symmetric part, i.e.,

$$\Re(W(N)) = W\left(\frac{1}{2}\left(N + N^T\right)\right).$$

The symmetric part of N has entries

$$\bar{n}_{ii} := n_{ii}, \quad \bar{n}_{ik} := -\frac{1}{2}|B_{ik}|(V_i^s + V_k^s),$$

where n_{ii} is defined in (31). From (37) it follows that

$$|B_{ii}|V_i^s > \sum_{k \sim \mathcal{N}_i} |B_{ik}|V_k^s.$$

Hence, together with (38) it follows that

$$|B_{ii}|V_i^s > \frac{1}{2} \sum_{k \sim \mathcal{N}_i} |B_{ik}|(V_i^s + V_k^s) = \sum_{k \sim \mathcal{N}\backslash\{i\}} |\bar{n}_{ik}|$$

and

$$\bar{n}_{ii} = 2|B_{ii}|V_i^s - \sum_{k \sim \mathcal{N}_i} |B_{ik}|V_k^s > |B_{ii}|V_i^s > \sum_{k \sim \mathcal{N}\backslash\{i\}} |\bar{n}_{ik}|.$$

Consequently, the symmetric part of N is diagonally dominant with positive diagonal entries and by Gershgorin's disc theorem its eigenvalues are all positive real. □□□

We are now ready to state our main result within this section.

Proposition V.5. *Consider the system* (12), (3)*. Fix D and positive real constants α and τ. Set $\tau_{P_i} = \tau$, $i \sim \mathcal{N}$ and $K = \kappa D$, where κ is a positive real parameter. Let $\mathrm{col}(V^s, Q^{m,s}) \in \mathbb{R}_{>0}^{2n}$ be the unique equilibrium point of the system* (12), (3) *corresponding to all $V(0)$ with the property $\|D^{-1}V(0)\|_1 = \alpha$. Denote by $x^s = \mathrm{col}(V_R^s, Q^{m,s}) \in \mathbb{R}_{>0}^{2n-1}$ the unique corresponding equilibrium point of the reduced system* (29), (27)*.*

Let $\mu_i = a_i + jb_i$ be the i-th nonzero eigenvalue of the matrix product $ND\mathcal{L}D$ with $a_i \in \mathbb{R}$ and $b_i \in \mathbb{R}$. Then, x^s is a locally exponentially stable equilibrium point of the system (29), (27) *if and only if the positive real parameter κ is chosen such that*

$$\tau \kappa b_i^2 < a_i \tag{39}$$

for all μ_i. Moreover, the equilibrium point x^s is locally exponentially stable for any positive real κ if and only if $N D \mathcal{L} D$ has only real eigenvalues.

Proof. We have just shown that with $\tau_{P_i} = \tau$, $i \sim \mathcal{N}$, the linear system (34) locally represents the microgrid dynamics (29), (27). The proof is thus given by deriving the spectrum of A, with A defined in (34). Let λ be an eigenvalue of A with a corresponding right eigenvector $v = \operatorname{col}(v_1, v_2)$, $v_1 \in \mathbb{C}^{n-1}$, $v_2 \in \mathbb{C}^n$. Then,

$$
\begin{aligned}
-\mathcal{L}_R D v_2 &= \lambda v_1, \\
\frac{1}{\tau}\left(N \mathcal{R} v_1 - v_2\right) &= \lambda v_2.
\end{aligned}
\tag{40}
$$

We first prove by contradiction that zero is not an eigenvalue of A. Therefore, assume $\lambda = 0$. Then,

$$
\mathcal{L}_R D v_2 = \underline{0}_{n-1}. \tag{41}
$$

From the definition of $\mathcal{L}_R$ given in (28) it follows that (41) can only be satisfied if

$$
K \mathcal{L} D v_2 = \begin{bmatrix} \underline{0}_{n-1} \\ a \end{bmatrix}, \quad a \in \mathbb{C}.
$$

The fact that $\mathcal{L} = \mathcal{L}^T$ together with $\mathcal{L} \underline{1}_n = \underline{0}_n$ implies that $\underline{1}_n^T K^{-1} K \mathcal{L} D v = 0$ for any $v \in \mathbb{C}^n$. Therefore,

$$
\underline{1}_n^T K^{-1} K \mathcal{L} D v_2 = \underline{1}_n^T K^{-1} \begin{bmatrix} \underline{0}_{n-1} \\ a \end{bmatrix} = \frac{a}{k_n} = 0.
$$

Hence, a must be zero. Consequently, $v_2 = \beta D^{-1} \underline{1}_n$, $\beta \in \mathbb{R}$. Inserting $\lambda = 0$ and $v_2 = \beta D^{-1} \underline{1}_n$ in the second line of (40) and recalling $K = \kappa D$ yields

$$
N \mathcal{R} v_1 = \beta D^{-1} \underline{1}_n = \beta \kappa K^{-1} \underline{1}_n. \tag{42}
$$

Premultiplying with $v_1^* \mathcal{R}^T$ gives, because of (36), $v_1^* \mathcal{R}^T N \mathcal{R} v_1 = 0$. As, according to the proof of Lemma V.4, $\Re(W(N)) \subseteq \mathbb{R}_{>0}$, this implies

$$
\mathcal{R} v_1 = \underline{0}_n. \tag{43}
$$

Hence, because of (42), $\beta = 0$ and $v_2 = \underline{0}_n$. Finally, because of (32), (43) implies $v_1 = \underline{0}_{n-1}$. Hence, (40) can only hold for $\lambda = 0$ if $v_1 = \underline{0}_{n-1}$ and $v_2 = \underline{0}_n$. Therefore, zero is not an eigenvalue of A.

We proceed by establishing conditions under which all eigenvalues of A have negative real part. Since $\lambda \neq 0$, (40) can be rewritten as

$$
\lambda^2 v_2 + \frac{1}{\tau} \lambda v_2 + \frac{1}{\tau} N \mathcal{R} \mathcal{L}_R D v_2 = \underline{0}_n. \tag{44}
$$

Recall from (35) that $\mathcal{R} \mathcal{L}_R = K \mathcal{L}$. Moreover, $K = \kappa D$. Hence, (44) is equivalent to

$$
\tau \lambda^2 v_2 + \lambda v_2 + \kappa N D \mathcal{L} D v_2 = \underline{0}_n. \tag{45}
$$

This implies that v_2 must be an eigenvector of $N D \mathcal{L} D$. Recall that Lemma V.4 implies that $N D \mathcal{L} D$ has a zero eigenvalue with geometric multiplicity one and all its other eigenvalues have positive real part. For $N D \mathcal{L} D v_2 = \underline{0}_n$, (45) has solutions $\lambda = 0$ and $\lambda = -1/\tau$. Recall that zero is not an eigenvalue of A. Hence, we have $\lambda_1 = -1/\tau$ as first eigenvalue (with unknown algebraic multiplicity) of the matrix A.

We now investigate the remaining $0 \leq m \leq 2n-2$ eigenvalues of the matrix $A \in \mathbb{R}^{(2n-1) \times (2n-1)}$. Denote the remaining[5] eigenvalues of $N D \mathcal{L} D$ by $\mu_i \in \mathbb{C}$. Let a corresponding right eigenvector be given by $w_i \in \mathbb{C}^n$, i.e., $N D \mathcal{L} D w_i = \mu_i w_i$. Without loss of generality, choose w_i such that $w_i^* w_i = 1$. By multiplying (45) from the left with w_i^*, the remaining m eigenvalues of A are the solutions $\lambda_{i_{1,2}}$ of

$$
\tau \lambda_{i_{1,2}}^2 + \lambda_{i_{1,2}} + \kappa \mu_i = 0. \tag{46}
$$

First, consider real nonzero eigenvalues, i.e., $\mu_i = a_i$ with $a_i > 0$. Then, clearly, both solutions of (46) have negative real parts, e.g., by the Hurwitz condition. Next, consider complex eigenvalues of $N D \mathcal{L} D$, i.e., $\mu_i = a_i + j b_i$, $a_i > 0, b_i \in \mathbb{R} \setminus \{0\}$. Then, from (46) we have

$$
\lambda_{i_{1,2}} = \frac{1}{2\tau}\left(-1 \pm \sqrt{1 - 4\tau\kappa(a_i + j b_i)}\right). \tag{47}
$$

We define $\alpha_i := 1 - 4 a_i \tau \kappa$, $\beta_i := -4 b_i \tau \kappa$ and recall that the roots of a complex number $\sqrt{\alpha_i + j\beta_i}$, $\beta_i \neq 0$, are given by $\pm(\psi_i + j\nu_i)$, $\psi_i \in \mathbb{R}$, $\nu_i \in \mathbb{R}$, [47] with

$$
\psi_i = \sqrt{\frac{1}{2}\left(\alpha_i + \sqrt{\alpha_i^2 + \beta_i^2}\right)}.
$$

Thus, both solutions $\lambda_{i_{1,2}}$ in (47) have negative real parts if and only if

$$
\sqrt{\frac{1}{2}\left(\alpha_i + \sqrt{\alpha_i^2 + \beta_i^2}\right)} < 1 \Leftrightarrow \sqrt{\alpha_i^2 + \beta_i^2} < 2 - \alpha_i.
$$

Inserting α_i and β_i gives

$$
\sqrt{(1 - 4 a_i \tau \kappa)^2 + 16 b_i^2 \tau^2 \kappa^2} < 1 + 4 a_i \tau \kappa,
$$

where the right hand side is positive. The condition is therefore equivalent to condition (39) for $b_i \neq 0$. Hence, A is Hurwitz if and only if (39) holds for all μ_i. Finally, x^s is locally exponentially stable if and only if A is Hurwitz [48]. $\square\square\square$

Remark V.6. *Note that equilibria of (29), (27) are independent of the parameters τ and κ. Hence, selecting κ according to the stability condition (39) does not modify a given equilibrium point $\operatorname{col}(V_R^s, Q_m^s)$.*

Remark V.7. *The selection $K = \kappa D$ is suggested in Proposition V.5 based on Lemma V.4, which states that $\Re\left(\sigma(N K L D)\right) \subseteq \mathbb{R}_{\geq 0}$ if $K = D$. This condition is sufficient, not necessary. Hence, there may very well exist other choices of K for which x^s, i.e., an equilibrium of the system (12), (3), is stable.*

VI. SIMULATION STUDY

The performance of the proposed DVC (8) is demonstrated via simulations based on the three-phase islanded Subnetwork 1 of the CIGRE benchmark medium voltage distribution network [49]. The network is a meshed network and consists

---

[5]Neither the algebraic multiplicities of the eigenvalues of the matrix product $N D L D$ nor the geometric multiplicities of its nonzero eigenvalues are known in the present case. However, this information is not required, since, to establish the claim, it suffices to know that $\Re(\sigma(N D L D)) \subseteq \mathbb{R}_{\geq 0}$. This fact has been proven in Lemma V.4.

of 11 main buses, see Fig. 2. To obtain a practically relevant setup, we assume that the phase angles of the inverters are controlled by the typical frequency droop control given in (5).

The main purpose of the simulation analysis is four-fold: *(i)* to evaluate the performance of the DVC (8) compared to the voltage droop control (7); *(ii)* to investigate the ability of the DVC to quickly achieve a desired reactive power distribution after changes in the load; *(iii)* to test the compatibility of the DVC (8) with the frequency droop control (5); *(iv)* to analyze the influence of control design parameters on convergence properties of the closed-loop system. These are main criteria for a practical implementation of the DVC (8). To this end, we have performed a large number of simulations with a variety of initial conditions, control parameters and load changes.

The network modeling follows [14]. Compared to the original system [49], the combined heat and power (CHP) diesel generator at bus 9b is replaced by an inverter-interfaced CHP fuel cell (FC). and the power ratings of the DG units are scaled by a factor 4, such that the controllable units (CHPs, batteries, FC) can satisfy the load demand in autonomous operation mode. We assume that the PV units connected at buses 3, 4, 6, 8 and 11 are not equipped with any storage device and, therefore, not operated in grid-forming, but in grid-feeding mode. This is standard practice and means that the PV units are controlled in such a way that they deliver a fixed amount of power to an energized grid [8]. Since then the PV units can not be represented by (4), we denote them as non-controllable units. Hence, the network in Fig. 2 possesses a total of six controllable DG sources. We assume that all these units are equipped with the frequency droop control given in (5). The voltage is controlled either by the DVC (8) or the voltage droop control (7), depending on the simulation scenario. We associate to each inverter its power rating S_i^N, $i \sim \mathcal{N}$ and assume for simplicity that the transformer power rating is equivalent to that of the corresponding generation source. The transformer impedances of the inverter-interfaced units are modeled based on the IEEE standard 399–1997 [50]. The corresponding shunt-admittance representing a load at a node is computed at nominal frequency and voltage and by summing the load demand and the PV generation at each node. Then, in the corresponding Kron-reduced network, all nodes represent controllable DGs. The line parameters and lengths are as given in [49]. As outlined in II-A, we merge the transformer and filter impedances of the inverters with the line impedances. The largest R/X ratio of an admittance in the network is then 0.3. For HV transmission lines it is typically 0.31 [8], [15]. Hence, the assumption of dominantly inductive admittances is satisfied. To satisfy Assumption V.1, the low pass filter time constants are set to $\tau_{P_i} = 0.2$ s, $i \sim \mathcal{N}$. For a European grid with nominal frequency $f^d = 50$ Hz, this is equivalent to $\tau_{P_i} = 10/f^d$.

All simulations are carried out in Plecs [51]. In contrast to the model given by (1), (4) used for the analysis, the inductances are represented by first-order ODEs in the model used for the simulations rather than constants as in (1). The graph model of the distributed communication network required for the implementation of the DVC (8) is also depicted in Fig. 2. Nodes that are connected with each other exchange their local reactive power measurements. Note that the communication is not all-to-all and that there is no central unit.

We consider the following representative scenario to illustrate our results: at first, the system is operated under nominal loading conditions; then, at $t = 0.5$ s there is a load increase at bus 9; at $t = 2.5$ s, the load at bus 4 is disconnected. The magnitude of each change in load corresponds to approximately $0.1S_{\text{base}}$. From a practical point of view, this represents a significant change in load. Furthermore, the total length of the power lines connecting bus 5 and 9, i.e., the two most remote nodes with grid-forming units, is 2.15 km with a total impedance of $0.014 + j0.005$ pu (without considering the transformers), where pu denotes per unit values with respect to the common system base power S_{base} given in Table I. Hence, the electrical distance between the buses is small and the requirement of reactive power sharing is practically meaningful in the considered scenario.

The gains and setpoints of the frequency droop controllers are selected according to the conditions given in (6), i.e., such that the inverters share the active power proportionally in steady-state. We select the nominal power rate of each source as weighting coefficient, i.e., $\gamma_i = S_i^N$, $i \sim \mathcal{N}$ and set $P_i^d = 0.6S_i^N$ pu, as well as $k_{P_i} = 0.2/S_i^N$ Hz/pu, $i \sim \mathcal{N}$.

Due to the lack of precise selection criteria for the reactive power setpoints and droop gains of the voltage droop control (7), we employ the criteria for frequency droop control given in (6), see also [12], [14]. To the best of our knowledge, this is standard practice. Hence, the droop gains of the voltage droop control (7) are set to $Q_i^d = 0.25S_i^N$ pu and $k_{Q_i} = 0.1/S_i^N$ pu/pu. For the DVC (8), we select the nominal power rate of each source as weighting coefficient, i.e., $\chi_i = S_i^N$, $i \sim \mathcal{N}$ (see also Remark III.3) and, following Proposition V.5, we select $K = \kappa D$ with $\kappa = 0.04$. For both voltage controls, we set $V_i^d = 1$ pu, $i \sim \mathcal{N}$.

The simulation results are shown for the system (4), (1) operated with the voltage droop control (7) in Fig. 3a and with the DVC (8) in Fig. 3b. The system quickly reaches a steady-state under both controls, also after the changes in load at $t = 0.5$ s and $t = 2.5$ s. Local stability of the reduced-dimension closed-loop voltage and reactive power dynamics under the control (8) is confirmed for all three operating points via Proposition V.5.

Under the voltage droop control (7), the reactive power is not shared by all inverters in the desired manner. Numerous further simulation scenarios confirm that the voltage droop control (7) does not achieve a desired reactive power sharing. From our experience, the relative deviations of the weighted reactive powers $\bar{Q}_i$, $i \sim \mathcal{N}$, in a steady-state, i.e., $\max_{i \sim \mathcal{N}} \bar{Q}_i^s / \min_{i \sim \mathcal{N}} \bar{Q}_i^s$, can be as low as a few percent, but also go beyond 30% for control parameters chosen within a practically reasonable range. Moreover, an increase in reactive power demand (see, e.g., the load step at $t = 0.5$ s), leads to an undesirable decrease of the voltage amplitudes. Therefore, [27], [32], [34] propose the use of a secondary control loop with an integrator to restore the voltage amplitudes to acceptable values.

On the contrary and as predicted, the DVC (8) does achieve a desired reactive power distribution in steady-state. Moreover,
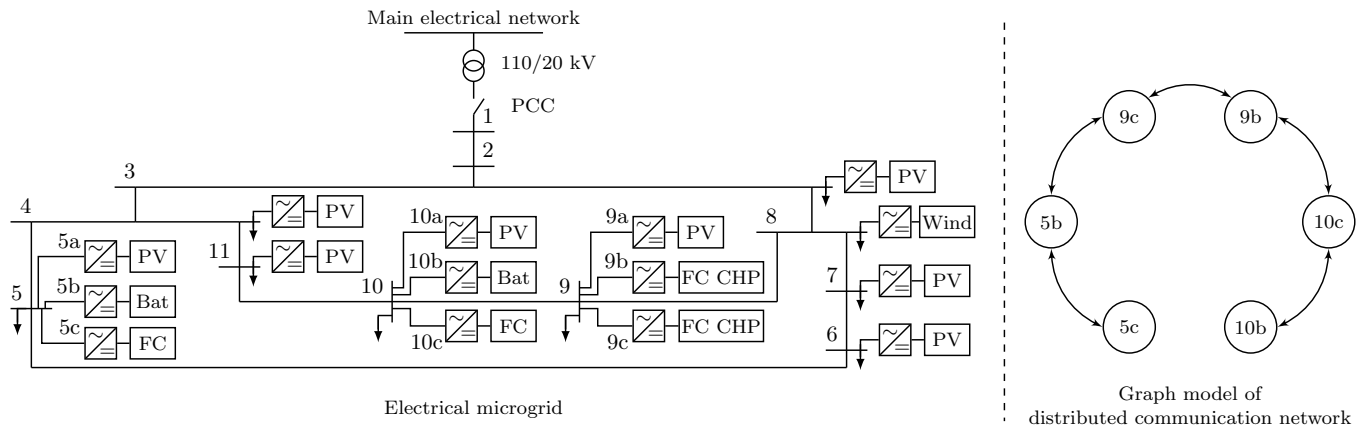
Fig. 2: 20 kV MV benchmark model adapted from [49] with 11 main buses and inverter-interfaced units of type: PV–photovoltaic, FC–fuel cell, Bat–battery, CHP fuel cell. The controllable units are located at buses 5b, 5c, 9b, 9c, 10b and 10c. PCC denotes the point of common coupling to the main grid. The sign ↓ denotes loads. The numbering of the main buses is according to [49].

when the system is operated with the DVC (8), the voltage levels remain close to the nominal value $V^d = 1$ pu. Also, as stated in Fact III.9, the average weighted voltage level remains constant for all $t \geq 0$ under the DVC (8), see Fig. 4. In addition, our simulation results show a good compatibility of the DVC (8) and the frequency droop control (5). As outlined in Section III-C, there exist other meaningful choices for K, for example, $K = \kappa I$. Overall, we have obtained the best performance with $K = \kappa D$ and $0.05 < \kappa < 0.15$.

Furthermore, κ is a very intuitive tuning parameter. In analogy to linear SISO control systems, low values of κ lead to relatively long settling times, but little overshoot. On the contrary, the larger κ is chosen, the shorter is the settling time at the cost of a higher overshoot and a broader error band. This effect is illustrated for different values of κ in Fig. 5. In addition, the convergence speed depends on the connectivity properties of the communication network, as well as on the physical characteristics of the electrical network. A detailed evaluation of the influence of these two points is subject of future research.

VII. CONCLUSION

We have proposed a distributed consensus-based voltage control, which solves the problem of reactive power sharing in inverter-based microgrids with dominantly inductive power lines. This problem is relevant in networks or network-clusters where the electrical distance between the generation units is small. Opposed to the widely used voltage droop control, see e.g., [9], the control presented here does guarantee a desired reactive power distribution in steady-state.

Moreover, under the assumption of small phase angle differences between the output voltages of the DG units, we have proven the following two statements: *(i)* the choice of the control parameters uniquely determines an equilibrium point of the voltage and reactive power dynamics; *(ii)* the control parameters and the time constants of the low-pass filters can be chosen such that this equilibrium point is locally exponentially stable.

TABLE I: Main test system parameters

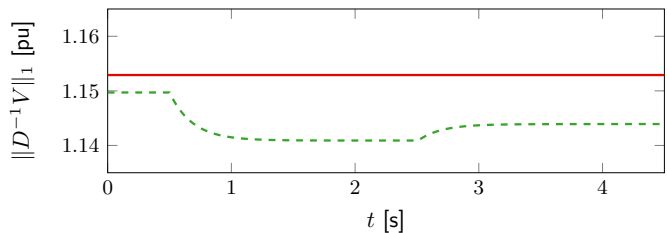| Base values	$S_{\text{base}} = 4.75$ MVA, $\quad V_{\text{base}} = 20$ kV
Max. sys. load	0.91+j0.30 pu
Total PV gen.	0.15 pu
S_i^N	$[0.505, 0.028, 0.261, 0.179, 0.168, 0.012]$ pu

Fig. 4: Weighted average voltage $\|D^{-1}V\|$ under the DVC (8) '–' and the voltage droop control (7) '- -' in pu.

The gain in performance in terms of power sharing compared to the usual voltage droop control has been demonstrated in a simulation example based on the CIGRE benchmark distribution network. In addition, the simulations show good compatibility of the proposed voltage control with the typical frequency droop control for inverters. We also have provided some intuition for the choice of the control parameters of the proposed DVC. Overall, the evaluation of the simulation results together with our experiences from numerous further simulation scenarios lead to the conclusion that the DVC is a well-suited control scheme for voltage control and reactive power sharing in inverter-based microgrids.

Future research will address relaxation of some of the assumptions and extend the analysis to microgrids with distributed rotational and electronic generation, i.e., with some sources interfaced to the network via SGs and others via inverters. In addition, the present analysis will be extended to network models with further, possibly dynamic, load models.
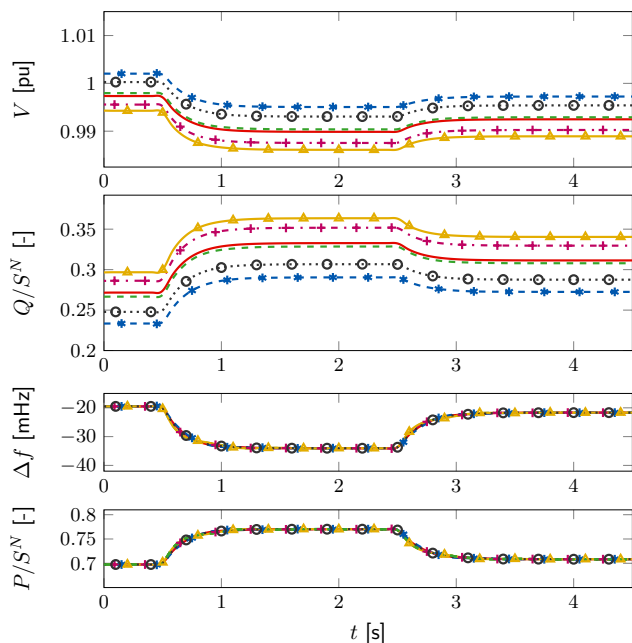
(a) Trajectories of the system (4), (1) under the frequency droop control (5) and the voltage droop control (7)
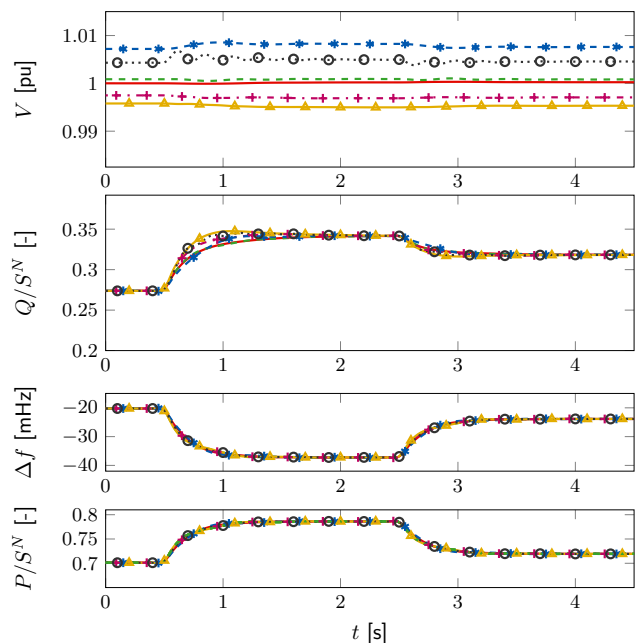
(b) Trajectories of the system (4), (1) under the frequency droop control (5) and the DVC (8)

Fig. 3: Comparison of voltage droop control and DVC. Trajectories of the power outputs relative to source rating P_i/S_i^N and Q_i/S_i^N, the voltage amplitudes V_i in pu and the internal relative frequencies $\Delta f_i = (\omega_i - \omega^d)/(2\pi)$ in Hz of the controllable sources in the microgrid given in Fig. 2, $i = 1, \ldots, 6$. The lines correspond to the following sources: battery 5b, $i = 1$ '–'; FC 5c, $i = 2$ '- -'; FC CHP 9b, $i = 3$ '+'; FC CHP 9c, $i = 4$ '* -'; battery 10b, $i = 5$ '△ -' and FC 10c, $i = 6$ 'o-'. The initial conditions have been chosen arbitrarily, but equal in both scenarios.
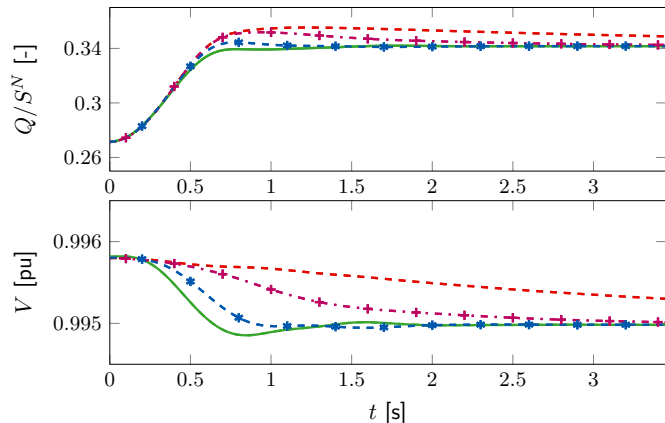

Fig. 5: Responses of the voltage amplitude V_5 and the weighted reactive power Q_5/S_5^N of inverter 5 at bus 10b to a load step at bus 9 for different values of κ : $\kappa = 0.005$ '- -', $\kappa = 0.02$ '+', $\kappa = 0.07$ '-*', $\kappa = 0.15$ '–'.

REFERENCES

[1] M. Chandorkar, D. Divan, and R. Adapa, "Control of parallel connected inverters in standalone AC supply systems," *IEEE Transactions on Industry Applications*, vol. 29, no. 1, pp. 136 –143, jan/feb 1993.

[2] R. Lasseter, "Microgrids," in *IEEE Power Engineering Society Winter Meeting, 2002*, vol. 1, 2002, pp. 305 – 308 vol.1.

[3] N. Hatziargyriou, H. Asano, R. Iravani, and C. Marnay, "Microgrids," *IEEE Power and Energy Magazine*, vol. 5, no. 4, pp. 78 –94, july-aug. 2007.

[4] H. Farhangi, "The path of the smart grid," *IEEE Power and Energy Magazine*, vol. 8, no. 1, pp. 18 –28, january-february 2010.

[5] T. Green and M. Prodanovic, "Control of inverter-based micro-grids," *Electric Power Systems Research*, vol. Vol. 77, no. 9, pp. 1204–1213, july 2007.

[6] J. Lopes, C. Moreira, and A. Madureira, "Defining control strategies for microgrids islanded operation," *IEEE Transactions on Power Systems*, vol. 21, no. 2, pp. 916 – 924, may 2006.

[7] F. Katiraei, R. Iravani, N. Hatziargyriou, and A. Dimeas, "Microgrids management," *IEEE Power and Energy Magazine*, vol. 6, no. 3, pp. 54–65, 2008.

[8] J. Rocabert, A. Luna, F. Blaabjerg, and P. Rodriguez, "Control of power converters in AC microgrids," *IEEE Transactions on Power Electronics*, vol. 27, no. 11, pp. 4734–4749, Nov 2012.

[9] J. Guerrero, P. Loh, M. Chandorkar, and T. Lee, "Advanced control architectures for intelligent microgrids – part I: Decentralized and hierarchical control," *IEEE Transactions on Industrial Electronics*, vol. 60, no. 4, pp. 1254–1262, 2013.

[10] P. Kundur, *Power system stability and control*. McGraw-Hill, 1994.

[11] N. Pogaku, M. Prodanovic, and T. Green, "Modeling, analysis and testing of autonomous operation of an inverter-based microgrid," *IEEE Transactions on Power Electronics*, vol. 22, no. 2, pp. 613 –625, march 2007.

[12] J. W. Simpson-Porco, F. Dörfler, and F. Bullo, "Synchronization and power sharing for droop-controlled inverters in islanded microgrids," *Automatica*, vol. 49, no. 9, pp. 2603 – 2611, 2013.

[13] J. Schiffer, R. Ortega, A. Astolfi, J. Raisch, and T. Sezi, "Conditions for stability of droop-controlled inverter-based microgrids," *Automatica*, vol. 50, no. 10, pp. 2457–2469, 2014.

[14] J. Schiffer, D. Goldin, J. Raisch, and T. Sezi, "Synchronization of droop-controlled microgrids with distributed rotational and electronic generation," in *52nd Conference on Decision and Control*, Florence, Italy, 2013, pp. 2334–2339.

[15] A. Engler, "Applicability of droops in low voltage grids," *International Journal of Distributed Energy Resources*, vol. 1, no. 1, pp. 1–6, 2005.

[16] Q.-C. Zhong, "Robust droop controller for accurate proportional load sharing among inverters operated in parallel," *IEEE Transactions on Industrial Electronics*, vol. 60, no. 4, pp. 1281–1290, 2013.

[17] Y. W. Li and C.-N. Kao, "An accurate power control strategy for power-electronics-interfaced distributed generation units operating in a low-voltage multibus microgrid," *IEEE Transactions on Power Electronics*, vol. 24, no. 12, pp. 2977 –2988, dec. 2009.

[18] J. W. Simpson-Porco, F. Dörfler, and F. Bullo, "Voltage stabilization in microgrids using quadratic droop control," in *52nd Conference on Decision and Control*, Florence, Italy, 2013, pp. 7582–7589.

[19] C. K. Sao and P. W. Lehn, "Autonomous load sharing of voltage source converters," *IEEE Transactions on Power Delivery*, vol. 20, no. 2, pp. 1009–1016, 2005.

[20] Y. Mohamed and E. El-Saadany, "Adaptive decentralized droop controller to preserve power sharing stability of paralleled inverters in distributed generation microgrids," *IEEE Transactions on Power Electronics*, vol. 23, no. 6, pp. 2806 –2816, nov. 2008.

[21] W. Yao, M. Chen, J. Matas, J. Guerrero, and Z.-M. Qian, "Design and analysis of the droop control method for parallel inverters considering the impact of the complex impedance on the power sharing," *IEEE Transactions on Industrial Electronics*, vol. 58, no. 2, pp. 576 –588, feb. 2011.

[22] C.-T. Lee, C.-C. Chu, and P.-T. Cheng, "A new droop control method for the autonomous operation of distributed energy resource interface converters," in *IEEE Energy Conversion Congress and Exposition (ECCE)*, 2010, pp. 702–709.

[23] K. Turitsyn, P. Sulc, S. Backhaus, and M. Chertkov, "Options for control of reactive power by distributed photovoltaic generators," *Proceedings of the IEEE*, vol. 99, no. 6, pp. 1063–1073, 2011.

[24] S. Bolognani and S. Zampieri, "A distributed control strategy for reactive power compensation in smart microgrids," *IEEE Transactions on Automatic Control*, vol. 58, no. 11, pp. 2818–2833, Nov 2013.

[25] S. Bolognani, G. Cavraro, R. Carli, and S. Zampieri, "A distributed feedback control strategy for optimal reactive power flow with voltage constraints," *arXiv preprint arXiv:1303.7173*, 2013.

[26] M. Marwali, J.-W. Jung, and A. Keyhani, "Control of distributed generation systems - part ii: Load sharing control," *IEEE Transactions on Power Electronics*, vol. 19, no. 6, pp. 1551 – 1561, nov. 2004.

[27] A. Micallef, M. Apap, C. Spiteri-Staines, and J. M. Guerrero, "Secondary control for reactive power sharing in droop-controlled islanded microgrids," in *IEEE International Symposium on Industrial Electronics (ISIE)*, 2012, pp. 1627–1633.

[28] R. Olfati-Saber, J. A. Fax, and R. M. Murray, "Consensus and cooperation in networked multi-agent systems," *Proceedings of the IEEE*, vol. 95, no. 1, pp. 215–233, 2007.

[29] H. Bouattour, J. W. Simpson-Porco, F. Dörfler, and F. Bullo, "Further results on distributed secondary control in microgrids," in *52nd Conference on Decision and Control*, Dec 2013, pp. 1514–1519.

[30] A. Bidram, A. Davoudi, F. L. Lewis, and Z. Qu, "Secondary control of microgrids based on distributed cooperative control of multi-agent systems," *IET Generation, Transmission & Distribution*, vol. 7, no. 8, pp. 822–831, 2013.

[31] A. Bidram, A. Davoudi, F. Lewis, and J. Guerrero, "Distributed cooperative secondary control of microgrids using feedback linearization," *IEEE Transactions on Power Systems*, vol. 28, no. 3, pp. 3462–3470, 2013.

[32] L.-Y. Lu, "Consensus-based P-f and Q-V droop control for multiple parallel-connected inverters in lossy networks," in *IEEE International Symposium on Industrial Electronics (ISIE)*, 2013, pp. 1–6.

[33] L.-Y. Lu and C.-C. Chu, "Autonomous power management and load sharing in isolated micro-grids by consensus-based droop control of power converters," in *1st International Future Energy Electronics Conference (IFEEC)*, Nov 2013, pp. 365–370.

[34] Q. Shafiee, J. Guerrero, and J. Vasquez, "Distributed secondary control for islanded microgrids – a novel approach," *IEEE Transactions on Power Electronics*, vol. 29, no. 2, pp. 1018–1031, 2014.

[35] J. Schiffer, T. Seel, J. Raisch, and T. Sezi, "A consensus-based distributed voltage control for reactive power sharing in microgrids," in *13th European Control Conference*, Strasbourg, France, 2014, pp. 1299–1305.

[36] H. Roger and R. J. Charles, *Topics in matrix analysis*. Cambridge University Press, 1991.

[37] C. Godsil and G. Royle, *Algebraic Graph Theory*. Springer, 2001.

[38] J. Machowski, J. Bialek, and J. Bumby, *Power system dynamics: stability and control*. J.Wiley & Sons, 2008.

[39] T. Van Cutsem and C. Vournas, *Voltage stability of electric power systems*. Springer, 1998, vol. 441.

[40] J. D. Glover, M. S. Sarma, and T. J. Overbye, *Power system analysis and design*. Cengage Learning, 2011.

[41] F. Dörfler and F. Bullo, "Kron reduction of graphs with applications to electrical networks," *IEEE Transactions on Circuits and Systems I: Regular Papers*, vol. 60, no. 1, pp. 150–163, 2013.

[42] E. Coelho, P. Cortizo, and P. Garcia, "Small-signal stability for parallel-connected inverters in stand-alone AC supply systems," *IEEE Transactions on Industry Applications*, vol. 38, no. 2, pp. 533–542, 2002.

[43] G. Diaz, C. Gonzalez-Moran, J. Gomez-Aleixandre, and A. Diez, "Scheduling of droop coefficients for frequency and voltage regulation in isolated microgrids," *IEEE Transactions on Power Systems*, vol. 25, no. 1, pp. 489 –496, feb. 2010.

[44] C. Hernandez-Aramburo, T. Green, and N. Mugniot, "Fuel consumption minimization of a microgrid," *IEEE Transactions on Industry Applications*, vol. 41, no. 3, pp. 673 – 681, may-june 2005.

[45] D. P. Bertsekas, A. Nedić, and A. E. Ozdaglar, *Convex analysis and optimization*. Athena Scientific Belmont, 2003.

[46] R. A. Horn and C. R. Johnson, *Matrix analysis*. Cambridge university press, 2012.

[47] S. Rabinowitz, "How to find the square root of a complex number," *Mathematics and Informatics Quarterly*, vol. 3, pp. 54–56, 1993.

[48] H. K. Khalil, *Nonlinear systems*. Prentice Hall, 2002, vol. 3.

[49] K. Rudion, A. Orths, Z. Styczynski, and K. Strunz, "Design of benchmark of medium voltage distribution network for investigation of DG integration," in *IEEE PESGM*, 2006.

[50] IEEE, "IEEE recommended practice for industrial and commercial power systems analysis (brown book)," *IEEE Standard 399-1997*, pp. 1–488, Aug 1998.

[51] Plexim GmbH, "Plecs software, www.plexim.com," 2013.